Structure and molecular dynamics of the mesophases exhibited by an organosiloxane tetrapode with strong polar terminal groups

D. Filip,[1,3] C. Cruz,[1,2,*] P. J. Sebastião,[1,2,†] and A. C. Ribeiro[1,2]
[1]*Centro de Física da Matéria Condensada, Av. Prof. Gama Pinto 2, 1649-003 Lisbon, Portugal*
[2]*IST, Department of Physics, Technical University of Lisbon, Av. Rovisco Pais, 1049-001 Lisbon, Portugal*
[3]*"Petru Poni" Institute of Macromolecular Chemistry, Aleea Gr. Ghica Voda 41 A, 700487-Iasi, Romania*

M. Vilfan[‡]
Jozef Stefan Institute, Jamova 39, SI-1000 Ljubljana, Slovenia

T. Meyer, P. H. J. Kouwer, and G. H. Mehl
Department of Chemistry, University of Hull, Cottingham Road, Hull HU6 7RX, United Kingdom
(Received 27 July 2006; published 16 January 2007)

The polymorphism of a new organosiloxane tetrapode compound with cyano terminal polar groups was characterized by means of polarizing optical microscopy and x-ray diffraction. The compound exhibits smectic-*A* and smectic-*C* phases with a partial bilayer arrangement due to a certain degree of head-to-head association of the mesogenic units through their cyano end groups. On the basis of x-ray diffraction results, evidencing the microsegregation of polyphilic molecules, packing models for the smectic-*A* and smectic-*C* phases are proposed. A high degree of smectic positional order and a relatively low value of the tilt angle in the smectic-*C* phase are indicated. Molecular dynamics of the studied compound was investigated by means of proton NMR relaxometry. The frequency dispersions of the spin-lattice relaxation time (T_1) show that the relaxation is induced by three rotational modes of individual dendrimer arms with frequencies between 10^6 and 10^9 Hz. In the smectic phases, the effect of individual rotations is overwhelmed by a well expressed contribution of layer undulations at Larmor frequencies below ~10 MHz. The appearance of this relaxation mechanism over the frequency range of three decades is so far unique in the case of thermotropic liquid crystals. The analysis of the layer undulations contribution supports the microsegregation model of the smectic phases by revealing a slowing-down of translational diffusion and the lack of interactions among the sublayers formed by the mesogenic groups.

DOI: 10.1103/PhysRevE.75.011704 PACS number(s): 61.30.−v, 76.60.−k

I. INTRODUCTION

Liquid crystalline (LC) dendrimers and structurally related multipodes constitute a fascinating class of materials with unusual physical properties due to their perfectly symmetrical branched structure resulting from a repetitive sequence of synthetic steps [1]. Supermolecules of this type are monodisperse and have, in general, an amorphous branched internal core and, on the periphery, mesogenic groups capable of forming anisotropic structures. The effect of the competition between opposite tendencies of the isotropic and anisotropic structural parts within the same molecule is of particular scientific interest. The isotropic dendritic architecture has a disordering influence on the packing of the mesogenic groups while the anisotropic mesogenic parts tend to self-organize into partially ordered structures. The coexistence of both isotropic and anisotropic structural parts in these systems leads to microsegregation inducing the formation of LC phases. Actually, the presence of mutually incompatible segments (for instance, aromatic core and aliphatic chains) in a single molecule is one of the main conditions potentially leading to the mesogenic character.

It is well known that monomeric organosiloxane compounds, composed of three different parts: aromatic, aliphatic, and siloxane, tend to segregate in three separate superposed sublayers [2–4]. The microsegregation of these incompatible moieties stabilizes the formation of layers and leads to the onset of smectic mesophases. In the case of polyphilic molecules, a simple comparison between the smectic period and the molecular length indicates the type of molecular organization within the smectic mesophase. However, a further detailed analysis based on the physical properties (such as effective dimensions, flexibility, and presence of electric dipolar moments) is necessary to describe accurately the packing of molecules in the smectic layers. In particular, the presence of a strong terminal electric dipole in the mesogenic core favors the occurrence of a rich polymorphism which may include several different types of smectic-*A* and smectic-*C* phases [5]. The appearance of such polymorphism originates from a competition between the tendency to the formation of smectic layers and the propensity of the cores to associate head-to-head due to the mutual electrostatic interaction of the terminal electric dipoles, leading to the so-called frustration mechanism. In the specific case of low molar mass organosiloxane LCs with cyanobiphenyl or other aromatic cores with strong terminal dipoles, the presence of nematic, partial bilayer smectic-*A* (SmA) and

*Electronic address: cruz@cii.fc.ul.pt
†Electronic address: pedros@lince.cii.fc.ul.pt
‡Electronic address: mika.vilfan@ijs.si

smectic-*C* (SmC) phases, and chiral smectic-*C* (SmC^*) phases was reported in the literature [2–4].

In the present study we are dealing with a zeroth generation organosiloxane dendrimer. It has four mesogenic cyanobiphenyl branches and is, therefore, called an organosiloxane tetrapode with polar terminal groups, shortly T-CN. The mesogenic groups are attached through flexible aliphatic spacers to the dendritic core. Such a compound combines the branching properties of dendrimers, the microsegregation effect typical of organosiloxane liquid crystalline compounds, and the frustration mechanisms due to the presence of terminal polar groups. The compound investigated exhibits the isotropic, SmA and SmC phases. The ratio between the smectic layers thickness and the molecular length in the SmA phase indicates the partial bilayer character of this mesophase, presumably due to the effect of the terminal cyano groups. The partial bilayer character of the SmC phase depends both on the layer thickness/molecular length ratio and on the tilt angle. The present work thus represents an extension of previous structural and molecular dynamics studies of low molar mass calamitic organosiloxane compounds. The increasing architectural complexity of dendrimer molecules opens new interesting problems which will be addressed in this paper. Namely, in dendrimer LCs not only the properties of individual mesogenes but also the overall shape and/or microsegregation determine the structure and dynamics of the mesophases formed through self-assembly [6–8].

In the present work, the effect of branching on the structural properties of the mesophases formed by the organosiloxane tetrapode is studied by the x-ray diffraction technique (XRD). In the low molar mass smectic phases with liquid-like layers, the usual x-ray diffraction patterns reflect one or more orders of pseudo-Bragg peaks in the low-angle region, resulting from quasi-long-range positional order of the smectic structure, and one or more superimposed diffuse bands corresponding to the short-range order defined by the average lateral distance between the different molecular moieties (aromatic, aliphatic, and siloxane). The knowledge of these parameters for T-CN, i.e., its layer thickness and lateral distances between molecular parts as well as their variation with temperature, is of crucial importance to reveal the structure and related molecular dynamics of dendrimer mesophases.

Proton nuclear magnetic resonance (NMR) relaxometry was applied to obtain an insight into molecular dynamics of T-CN in a broad frequency range. A large domain of Larmor frequencies from $\sim$10 kHz to 300 MHz was accessed by measuring the frequency dependence of spin relaxation times using the combined standard and fast field-cycling NMR techniques. The analysis of experimental results in terms of different relaxation mechanisms yields characteristic times related to local and collective molecular reorientations. Dielectric spectroscopy of a similar dendritic compound indicated a considerable slowing down of molecular dynamics compared to the monomeric LCs [9]. As a matter of fact, in T-CN the slowing down of translational diffusion gives rise to a clear observation of collective orientational fluctuations in contrast to monomeric smectic phases where collective fluctuations are hardly observable by NMR. An assessment of molecular dynamics in T-CN may also contribute to the clarification of particular questions concerning the structural properties of the mesophases under study [10].

The disposition of the paper is as follows. In Sec. II we describe the experimental techniques used in the present study, i.e., polarizing optical microscopy, x-ray diffraction measurements, and proton NMR relaxometry. There follows a description of the chemical structure of T-CN and its phase transitions as determined by polarizing optical microscopy and differential scanning calorimetry. In the first part of Sec. III we analyze the x-ray diffraction data. Including the calculated distances from molecular modeling, the information on the structure of smectic phases is obtained. A high degree of positional smectic order in the SmA phase and a low tilt angle in the SmC phase are indicated. In the second part of Sec. III, we present the measurements of the proton spin-lattice relaxation times in the Larmor frequency range between $\sim$10 kHz and 300 MHz. The fitted parameters related to the characteristic time constants are discussed and the NMR observation of layer undulations is pointed out. A comparison between the results of this study and those obtained for more conventional calamitic LCs is made. A summary is given in Sec. IV.

II. EXPERIMENT

A. Experimental techniques

Polarizing optical microscopy observations of T-CN were performed using an Olympus BH polarizing microscope, equipped with a Mettler FP 5 hot stage. Maximal heating/cooling rates on observing the samples were 3 K/min.

X-ray diffraction measurements on aligned samples were performed on a MAR345 diffractometer with a 2D image plate detector (Cu Kα radiation, graphite monochromator, $\lambda = 1.54$ Å). The samples were heated in the presence of a magnetic field using a home-built capillary furnace.

The proton spin-lattice relaxation times, T_1, were obtained using three different spectrometers in order to cover a broad frequency range from 10 kHz to 300 MHz. T_1 measurements at Larmor frequencies between 10 kHz and 1 MHz were performed using a home built fast field-cycling spectrometer [11] with a polarization and detection field of 0.215 T (corresponding to the Larmor frequency of 9.1 MHz) and switching times of 2–3 ms. The T_1 data between 4 and 100 MHz were obtained with a conventional pulsed NMR spectrometer BRUKER SXP 4-100 using the inversion-recovery rf pulse sequence with phase cycling $[(\pi)_x - (\pi/2)_{x,-x}]$ for suppression of the DC bias. Finally, a Bruker MSL 300 was used for the measurements at 300 MHz. The NMR samples consisted of a few hundred milligrams of the LC material sealed under moderate vacuum ($<10^{-4}$ Torr) in NMR glass tubes. All the measurements were performed after slowly cooling the sample at a rate lower than 1 K/min in the presence of the external magnetic field, from a temperature in the isotropic phase to the desired temperature. The temperature was controlled within ±0.5 °C. The magnetization (observed through the amplitude of the FID signals) showed mono-exponential time-dependence suggesting that a uniform T_1 is established in the sample. The experimental error of spin-lattice relaxation measurements is estimated to

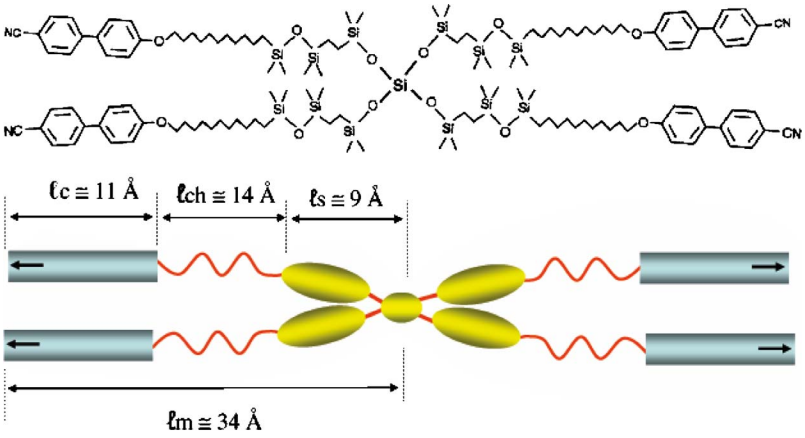

g -25°C→ Cr 38°C→ SmC 49°C→ SmA 82°C→ I

FIG. 1. (Color online) Schematic representation of the organosiloxane tetrapode T-CN molecule, its chemical formula, and phase sequence. Molecular dimensions of T-CN resulting from molecular modeling: ℓ_m–length of the dendrimer arm; ℓ_c–length of the cyanobiphenyl mesogenic group; ℓ_{ch}–length of the aliphatic chain; ℓ_s–length of the siloxane chain. An extended configuration of the molecule has been assumed in the modeling.

be less than ±10%. It is interesting to note that the sample was partly oriented by the magnetic field as revealed from the angular dependence of proton NMR spectra on rotating the sample.

B. Description of the studied system

The compound under study is an organosiloxane tetrapode with molecular mass 2071.9 g/mol which contains a siloxane core and biphenyls as mesogens with cyano polar terminal groups. This oligomer is a generation 0 dendrimer and it was synthesized as described in [12]. The mesogenic unit is linked to the central Si atom through 1,1,3,3-tetramethyldisiloxane groups and long flexible spacers of eleven methylene groups. The chemical structure of the compound, shortly referred as T-CN, the phase sequence and transition temperatures are presented in Fig. 1.

The phase sequence of T-CN was characterized by polarizing optical microscopy (POM), differential scanning calorimetry (DSC), and x-ray diffraction. POM observations revealed characteristic textures for the SmA and SmC phases. In Fig. 2 we present four textures obtained by POM of T-CN under different conditions. In Figs. 2(a) and 2(b) fan-shaped and broken fan-shaped textures—typical of SmA and SmC phases, respectively—can be observed. During the optical observation, the T-CN sample was also submitted to a shearing process. In Figs. 2(c) and 2(d) the textures obtained after shearing are shown. In Fig. 2(c) the fan-shaped patterns corresponding to SmA phase are still observed together with the black regions characteristic of homeotropic alignment. After a slow cooling, the transition into the smectic-*C* phase is

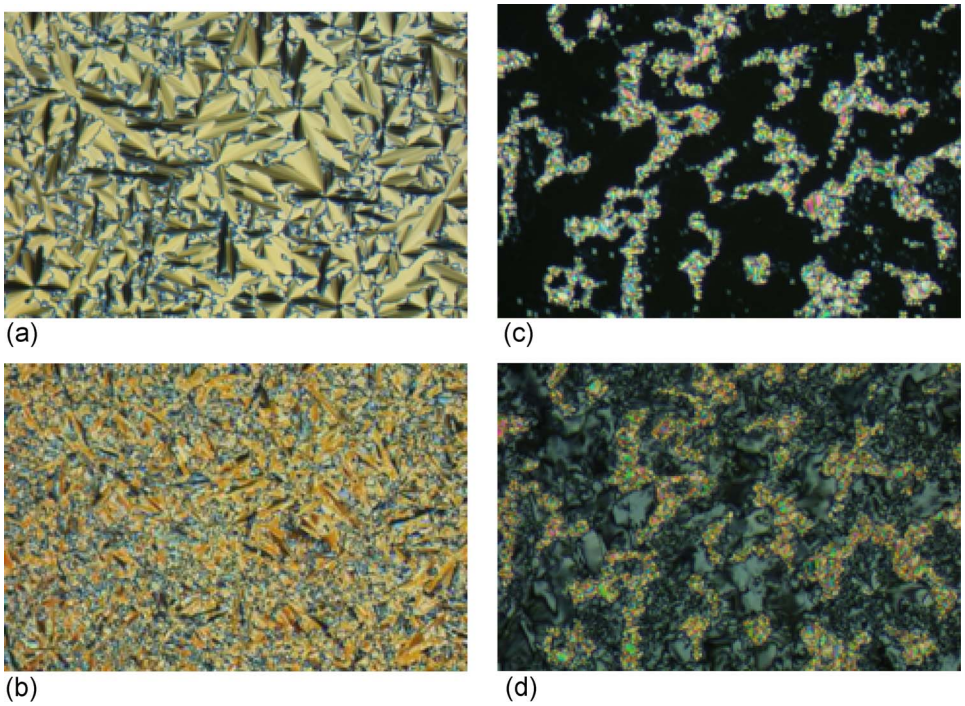

FIG. 2. (Color online) Textures observed for T-CN: (a) SmA phase, 70 °C, fan-shaped texture; (b) SmC phase, 35 °C, broken fan-shaped texture; (c) SmA phase, 60 °C, after shearing, fan-shaped texture together with homeotropic regions; (d) SmC phase, 45 °C, after shearing, broken fan-shaped texture together with schlieren textures.

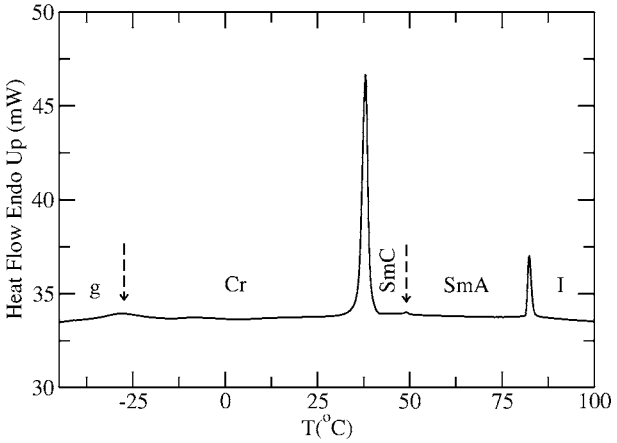

FIG. 3. DSC diagram for heating scans of the T-CN compound.

detected. Below the transition the fan-shaped patterns became broken fan-shaped and the black regions became grey [see Fig. 2(d)] which suggests small molecular tilting with respect to a direction normal to the glass plates. The transition temperatures obtained by POM are consistent with the DSC results (Fig. 3).

The structural characteristics of the T-CN molecule, such as the type of internal core, the spacer length, and the type of the mesogenic group, influence its physico-chemical behavior. The long flexible spacer of eleven methylene units assures a strong decoupling of the anisotropically orientable mesogenic groups from the core. The peripheral mesogenic groups have freedom to develop ordered structures and the polymorphism of the system becomes similar to the one of low molecular weight LCs. Actually, the appearance of smectic phases was expected in analogy with the side-chain liquid crystal polymers, where a longer spacer influences the degree of anisotropic LC ordering from nematic to the smectic and also the formation of crystalline phases [13].

III. RESULTS AND DISCUSSION

A. Structural characterization

Two-dimensional x-ray diffraction patterns obtained in the temperature range of the SmA and SmC phases of the aligned T-CN sample clearly show the characteristics of layered structures. In Fig. 4(a) we present the two-dimensional x-ray diffraction pattern recorded in the SmA phase at 50 °C. The corresponding azimuthally integrated XRD pattern (intensity versus scattering vector magnitude, $q=4\pi\sin(\theta)/\lambda$) is presented in Fig. 4(b).

Similar x-ray diffraction patterns and intensity profiles were obtained at other temperatures both for the SmA and SmC phases. All profiles are characteristic of a smectic state with one-dimensional positional order and liquid-like organization within the layers. First, the two sharp peaks in the small angle region correspond to the first and second order pseudo-Bragg reflections associated with smectic layers of thickness $\ell \simeq 48$ Å. The two sharp peaks are well fitted by two Lorentzian curves as shown in Fig. 4(b). The fact that

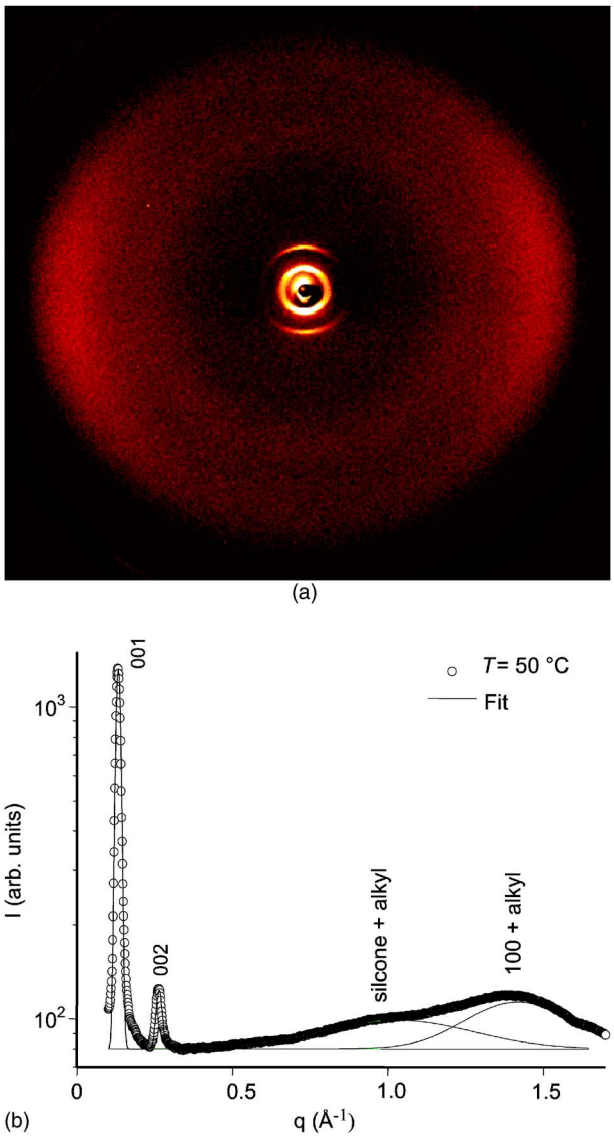

FIG. 4. (Color online) (a) Two dimensional x-ray diffraction pattern for T-CN in the SmA phase at 50 °C. (b) Fit of the azimuthally integrated x-ray pattern [intensity vs scattering vector magnitude, $q=4\pi\sin(\theta)/\lambda$] for T-CN in the SmA phase at 50 °C.

the second order diffraction line is clearly seen reflects a rather high degree of smectic order in the sample. At wide angles, a broad asymmetric diffused band can be fitted by a superposition of two broad Gaussian curves as shown in Fig. 4(b). These bands are related to the disordered in-plane arrangement of the molecules within the smectic layer. The diffuse band at ~4.4 Å corresponds to the lateral distance associated with the liquid-like positional order of the alkyl chains and aromatic cores within the layers, where it should be stressed that the orientational order of the aromatic cores is much larger than that of the chains. Another diffuse band at about ~6.1 Å corresponds to the liquid-like in-plane arrangement of the siloxane moieties. The characteristic distances resulting from the fitting of the x-ray pattern are presented in Table I.

In Fig. 5 we present the layer spacing ℓ, obtained from the integrated x-ray profiles, as a function of temperature. As

TABLE I. Fitted parameters obtained for the azimuthally integrated X-ray pattern of T-CN registered in the SmA phase at 50 °C.

Diffraction peaks	Distance (Å) ($2\pi/q$)
001	48.0
002	
siloxane	6.1
alkyl+aromatic	4.4

shown in the figure, the layer spacing in the SmA phase increases linearly (within the experimental error) with decreasing temperature, from 44 Å at I-SmA transition to about 48 Å at the SmA-SmC transition. The increasing in the layer spacing clearly slows down below the SmA-SmC transition.

In the following we present a model for the molecular organization of the T-CN smectic phases, taking into account the x-ray diffraction results (Figs. 4 and 5) and the T-CN molecular structure (Fig. 1). We see that each dendrimer arm is composed of a siloxane chain attached to the central Si atom, an alkyl chain, and an aromatic mesogenic core. The aromatic core and the alkyl chain can be considered as a mesogenic unit. The values presented in Fig. 1 correspond to approximate dimensions where the chains' lengths are estimated for an extended (planar zig-zag) configuration. Actually, the melting of the chains in the SmA and SmC phases induces the presence of many different configurations. As can be expected, these configurations are not considered individually but will be interpreted in terms of average molecular volume and cross-sectional areas as described below.

The experimental value of the T-CN layer thickness is 48 Å at ~50 °C and the corresponding ratio $\ell/\ell_m \sim 1.4$ [ℓ_m is the length of an extended dendrimer arm corresponding to a monomer (see Fig. 1)]. This value indicates a partially bilayered arrangement for the smectic phases. According to models presented in the literature, the layers in the ordinary bilayer SmA phase are formed by a mixture of single molecules (corresponding to the monomers in our case) and dimers, the latter constituted by pairs of molecules associated head-to-head through their strong polar end groups [14]. The relative size of those populations determines the layer spacing. Taking into account the chemical structure of the tetrapode and, in particular, the linking of the mesogenic arms to the central siloxane core, it is reasonable to expect an up-and-down arrangement of the mesogenic units with respect to the siloxane in agreement with the basic steric and entropic requirements (see Fig. 6). Considering such an up-and-down molecular arrangement of the mesogenic arms and mutual incompatibility of their constituent parts, a microsegregated structure is indicated on the basis of x-ray diffraction data with smectic layers consisting of a mixture of:

(i) mesogenic units forming a dimer by head-to-head association with other mesogenic units belonging to the nearest tetrapode from the neighboring layer,

(ii) mesogenic units which remain unpaired in the smectic layer and retain the monomeric character.

The result is a partially bilayered structure as indicated by the ratio ℓ/ℓ_m. Such a structure is in agreement with the growing of the layer spacing with decreasing temperature (Fig. 5). The growing is explained by the diminishing of the chain melting degree with decreasing temperature. Moreover, in the partially bilayered system, a possible increase in the degree of head-to-head association with decreasing temperature also contributes to the increasing thickness of smectic layers [15]. Somewhat unexpectedly, the layer spacing in the SmC phase also increases with decreasing temperature, though only slightly. One possible explanation of this effect can be attributed to the competition between the expected decreasing of layer spacing resulting from the tilting of the molecules and increasing of molecular length due to the increasingly extended conformation of the aliphatic chains. In addition, it must be taken into account that a higher degree of dimers association at lower temperatures would also correspond to a larger layer spacing. The slight increasing in the layer spacing in the SmC phase therefore points out the prevailing effect of chain stiffening over the tilting and, consequently, a low value of the tilt angle. Actually, the tilting occurs most probably only in the sublayers formed by the mesogenic units. Therefore, it does not induce a drastic diminishing in the thickness of the whole layer, and does not promote the development of the chevron structure in the aligned sample. This conjecture is corroborated by the lack of the four Bragg diffraction peaks at small angles which are typically observed in 2D x-ray diffraction patterns of the ordinary smectic-*C* phases.

In order to get a further insight into the molecular organization of the T-CN smectic phases, it is necessary to calculate the molecular area. The molecular area is defined as $\Sigma = V_m/\ell$, where V_m is the molecular volume and ℓ is the layer spacing. V_m can be estimated from the molecular mass and density. Considering that the density of this type of materials is close to 1 g cm^{-3}, this value can be used as a first approximation to estimate the molecular volume of the tetrapode yielding $V_m \sim 3400$ Å^3.

For the sake of clarity, the phase structure is discussed by considering a pair of mesogenic arms belonging to two neighboring tetrapodes from subsequent layers as the basic unit of a smectic layer. According to the packing model proposed above, each of the mesogenic units [consisting of aromatic moiety and long aliphatic chain (see Fig. 6)] is connected to the corresponding dendrimer core, located on a

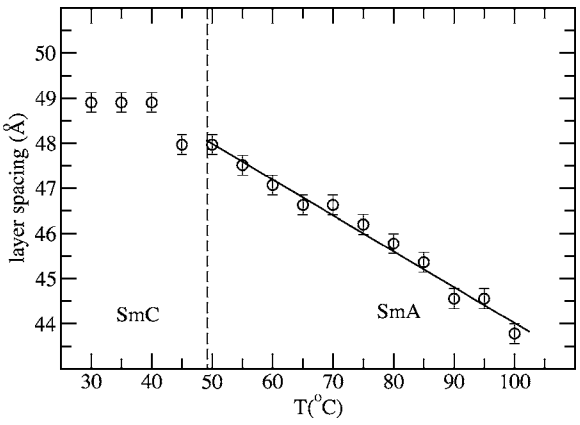

FIG. 5. Variation of the layer spacing in the SmA and SmC phases as a function of temperature.

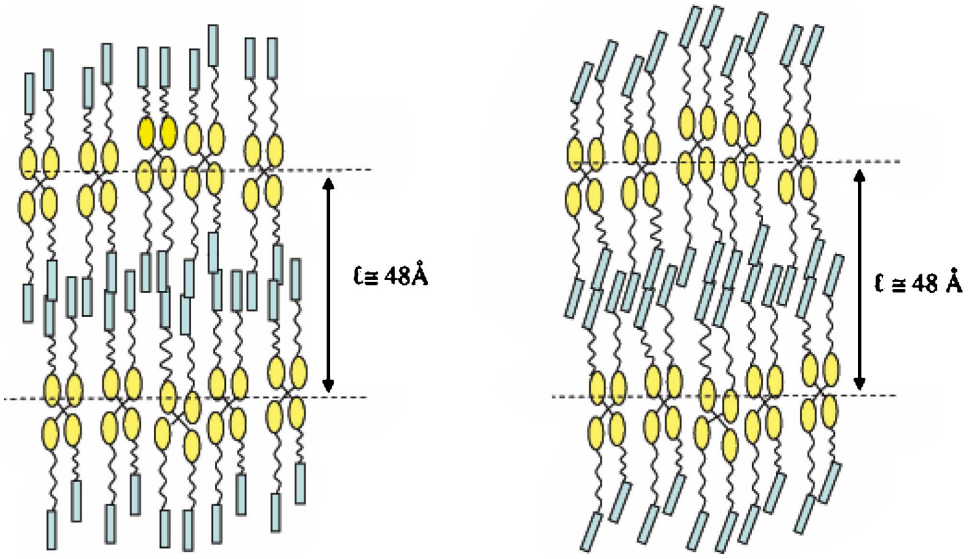

FIG. 6. (Color online) Proposed packing models for the SmA (a) and SmC phases (b).

siloxane sublayer formed by the microsegregation effect. The resulting molecular area for a pair of mesogenic arms in the layer is then $\Sigma_1=\Sigma/2=V_m/2\ell\sim 36$ Å^2 at about 47 °C. This value is close to that found for the partial bilayer SmA phases of low molar mass siloxane compounds bearing cyano end groups [4,15]. The magnitude of the estimated $\Sigma_1 \sim 36$ Å^2 is between one and two times cross-sectional area of the aromatic core σ_{ar}, which is about 22 Å^2 [15] in agreement with the square of the lateral distance between aromatic cores obtained from the x-ray intensity profile. This fact clearly corroborates the assumption of a partially bilayered arrangement of the aromatic cores. It is worthwhile to recall that the molecular area corresponding to a pair of mesogenic units, Σ_1, would be approximately the cross-sectional area σ_{ar} for an ideal bilayer SmA arrangement and about twice this cross-sectional area for a smectic layer consisting of unpaired mesogenic units only. In the partially bilayered SmA phase the fraction of the head-to-head molecular pairs, i.e., dimers, is $\tau\simeq 2-\Sigma_1/\sigma_{ar}$ [4], which amounts in the case of T-CN to ~0.37. It should be stressed that, according to the molecular organization described above, the three constituent parts of the T-CN molecules (aromatic, aliphatic, and siloxane) segregate into separate sublayers as previously observed in low molar mass organosiloxane LC systems.

For the paraffinic sublayer, the cross sectional area σ_{ch} can vary between 20 and 40 Å^2 depending on the chain conformation [15]; therefore, the above Σ_1 value is consistent with a partially bilayered arrangement with prevailing nonpaired mesogenic units. As for the siloxane sublayers, Σ_1 is compatible with the value of ~37 Å^2 for the square of the average lateral distance between the siloxane groups as determined from the x-ray data (see Table I). This value is somewhat smaller than the transverse size of the bulky siloxane groups of nearly globular shape [16] (≃43 Å^2), suggesting a double layered arrangement with some of the siloxane groups partially included amongst the disordered aliphatic chains [4]. In fact, the partial bilayered arrangement of the phase can be interpreted as a result of a strong competition between the tendency to the head-to-head association of the cyano terminal groups (leading to a decrease of the molecular coverage Σ_1) and the opposite steric effect of the siloxane groups which tend to segregate into distinct sublayers [15].

The proposed packing model for the SmA phase [Fig. 6(a)] is in line with that proposed for a low molecular weight organosiloxane liquid crystal similar to the mesogenic arm of the T-CN compound [15].

As for the molecular packing in the SmC phase, the most probable picture is the one in which only the mesogenic units are tilted. If one takes into account the values of layer spacing which are similar or larger than those in the SmA phase and also a very low transition enthalpy estimated from the DSC peak, it is most likely that the molecular packing within the smectic-*C* phase is almost the same as in the SmA phase with a small tilt angle of the mesogenic cores with respect to the layers [Fig. 6(b)].

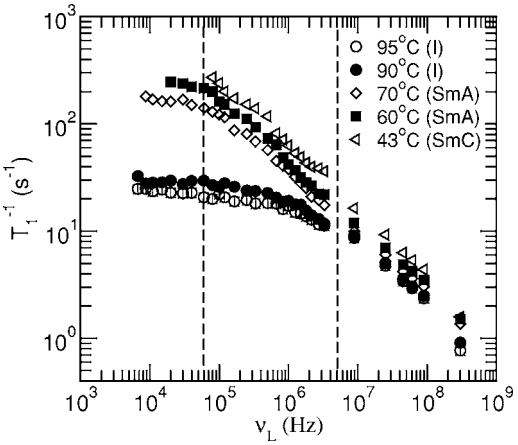

FIG. 7. Frequency dispersions of the proton spin-lattice relaxation rate T_1^{-1} in the isotropic, SmA, and SmC phases of T-CN. In the frequency range between the dashed vertical lines the relaxation rate in the smectic phases shows a much stronger frequency dispersion ($T_1^{-1}\sim\nu_L^{-1}$) than in the isotropic phase. This effect is ascribed to the undulations of mesogenic smectic sublayers. Above ~10 MHz smectic and isotropic phases exhibit almost identical frequency dependence caused by intra-molecular reorientations.

B. Molecular dynamics

1. Experimental results

The proton spin-lattice relaxation rates, T_1^{-1}, measured as a function of Larmor frequency in the isotropic, smectic-*A*, and smectic-*C* phases of T-CN, are presented in Fig. 7.

The random error limits are estimated to be ±10% but, for the sake of the clearness of the graphs, the error bars are omitted. As seen in the figure, a regular monotonic decrease of T_1^{-1} with increasing frequency is detected for all phases in the frequency range above 10 MHz. For a given frequency above 10 MHz, the spin-lattice relaxation rate decreases with increasing temperature as observed in many low molar mass liquid crystals. For frequencies below ~10 MHz, two different types of dispersion can be noticed. The spin-lattice relaxation rate in the isotropic phase is nearly frequency independent. A similar behavior has been found in more conventional calamitic LCs [17,18]. On the other hand, in the SmA phase a strong increasing in T_1^{-1} with decreasing frequency—almost linear in ν_L^{-1}—is seen in the frequency range between ~100 kHz and ~10 MHz. This phenomenon is in strong contrast to the T_1^{-1} dispersion in low molar mass smectic phases where an almost frequency independent plateau appears in the same frequency range. Below ~100 kHz, a leveling-off in the T-CN dispersion curve is observed leading to a plateau at the lowest frequencies. A similar T_1^{-1} dispersion has been recorded in the SmC phase, but the expected leveling-off at low frequencies could not be detected due to the limiting conditions of the spectrometer used in the present study.

2. Relaxation mechanisms and models

In order to perform a quantitative analysis of the observed relaxation rates, it is necessary to consider which dynamic processes and associated relaxation mechanisms could account for the frequency and temperature dependencies of T_1^{-1} in all phases. In low molecular weight LC, the T_1^{-1} dispersion above 10 MHz and its temperature variation are usually associated with fast, thermally activated rotations/reorientations and translational self-diffusion of molecules. Below 10 MHz the spin-lattice relaxation dispersions become more sensitive to the structure and dynamics of a particular mesophase. For example, in the nematic phase the spin-lattice relaxation rate is proportional to the inverse square root of the Larmor frequency ν_L, i.e., $T_1^{-1} \propto \nu_L^{-1/2}$ [17,18]. The underlying relaxation mechanism is associated with three-dimensional collective orientational fluctuations of molecules, known as order director fluctuations (ODF). The divergence of the spin-lattice relaxation rate in the low frequency limit is avoided by the cut-off of long wavelength director modes and/or by the local field effect [19]. In the SmA phase, a linear dispersion $T_1^{-1} \propto \nu_L^{-1}$ would be expected due to the two-dimensional character of layer undulations (LU) which are the only collective orientational fluctuations supported by the layered structure of the smectic phases. However, at intermediate frequencies between 10 kHz and 10 MHz, the relaxation in the calamitic smectic-*A* phase is still strongly influenced by the relatively slow translational self-diffusion, marked by a plateau in the dispersion curve and masking the effect of layer undulations. Therefore, the strong dispersion $T_1^{-1} \propto \nu_L^{-1}$ has only been observed below ~10 kHz [20–22], and even then, doubts were raised whether NMR relaxometry truly detects layer undulations. On one side, the reliability of experimental data below ~10 kHz was questioned [23], and on the other, the damping effect of the possible interactions between layers, leading to a dispersion of logarithmic type, was theoretically pointed out [24].

As mentioned above, the analysis of the relaxation data in low molar mass LCs usually comprises three relaxation mechanisms, which are effective by modulating the intra- and intermolecular proton dipolar interactions. These are (i) local molecular rotations/reorientations, (ii) molecular translational self-diffusion, and (iii) collective orientational fluctuations. In view of different time scales of these processes, the total relaxation rate is given as the sum of contributions of different relaxation rates [17,25]. In the case of T-CN, the above relaxation mechanisms are affected by the specific structure of the system: due to the micro-segregation effect in the smectic phases the mesogenic aromatic moieties are arranged in well-defined sublayers, they are linked to the central siloxane core by the long flexible alkyl chains, and the interdigitation of mesogenic units into the neighboring layers takes place.

(i) Local molecular reorientations in dendrimer tetrapodes are slower than in monomeric LCs as shown by recent dielectric measurements. Dielectric spectroscopy covers the frequency range from ~1 Hz up to ~10 MHz and reveals in a tetrapode, similar to T-CN, a slowing down of local molecular dynamics by several orders of magnitude compared to the low molar mass counterparts [9]. In the tetrapode systems it is reasonable to assume the existence of both slow global molecular reorientations and faster rotations/reorientations of individual mesogenic arms of the tetrapode. Their dynamics comprises conformational changes and reorientations both about the long and short axes of the dendrimer branches. The flexibility of the long alkyl chains, connecting the aromatic units to the dendrimer core, permits at least a partial decoupling of the motion of mesogenic cores.

(ii) Molecular translational self-diffusion in T-CN is expected to be considerably slower than in the monomeric compounds. In the isotropic phase, the increased molecular mass and the branched structure hamper translational displacements. In the smectic phases, the inter-connection and inter-digitation of mesogenic cores should result in strong restrictions to the molecular translational displacements. Nevertheless, possible global displacements of the tetrapodes center of masses, resulting from successive random reorientations of the individual tetrapode arms, cannot be excluded. For this mechanism, no specific relaxation model could be found in the literature.

(iii) In spite of the complex molecular structure of the tetrapode the smectic layers are well defined as the result of the microsegregation of molecule's distinct noncompatible chemical groups. The collective fluctuations in the form of layer undulations are therefore expected to contribute to the spin-lattice relaxation in the kHz frequency range.

In the analysis of T-CN experimental data, a simple relaxation model consisting of a sum of Bloembergen-Purcell-

Pound (BPP) relaxation rates plus a relaxation rate contribution of layer undulations (LU) will be used,

$$\left(\frac{1}{T_1}\right) = \sum_i \left(\frac{1}{T_1}\right)_{\mathrm{BPP}_i} + \left(\frac{1}{T_1}\right)_{\mathrm{LU}}. \quad (1)$$

The BPP-type of relaxation rate is appropriate to describe a simple reorientation process with the characteristic correlation time τ_i and is given by the expression

$$\left(\frac{1}{T_1}\right)_{\mathrm{BPP}_i}(\nu_L, A_{\mathrm{ROT}_i}, \tau_i) = A_{\mathrm{ROT}_i}\left[\frac{\tau_i}{1+4\pi^2\nu_L^2\tau_i^2} + \frac{4\tau_i}{1+16\pi^2\nu_L^2\tau_i^2}\right], \quad (2)$$

where $A_{\mathrm{ROT}i}$ is a constant depending on the strength of interproton magnetic dipolar interactions. The temperature dependence of the correlations times τ_i is described by the Arrhenius law in the form

$$\tau_i = \tau_{i,\infty} e^{W_i/k_B T}, \quad (3)$$

where W_i are the activation energies and T is absolute temperature.

Since the tilt angle in the smectic-C phase is very small, layer undulations in both smectic-A and C phases are described by

$$\left(\frac{1}{T_1}\right)_{\mathrm{LU}}(A_{\mathrm{LU}}, \nu_L, \nu_{c\ \max}, \nu_{c\ \min}) = A_{\mathrm{LU}}\frac{2}{\pi\nu_L}\left[\arctan\left(\frac{\nu_{c\ \max}}{\nu_L}\right) - \arctan\left(\frac{\nu_{c\ \min}}{\nu_L}\right)\right], \quad (4)$$

where A_{LU} is a constant which depends on the viscoelastic properties of the material, and $\nu_{c\ \max}$ and $\nu_{c\ \min}$ are the high and low cut-off frequencies of director fluctuations given by $K_1 q_{\max}^2/(2\pi\eta)$ and $K_1 q_{\min}^2/(2\pi\eta)$, respectively [21,26]. K_1 denotes the splay elastic constant and η the corresponding viscosity. The contribution of translational self-diffusion has not been included in Eq. (1). A brief inspection of the dispersion curves in the smectic phases, namely, shows that the diffusion-induced plateau, expected between ~100 kHz and a few MHz, is missing. This supports the conjecture that the translational diffusion of the tetrapode is too slow to be effective in the frequency range accessible to NMR relaxation measurements. Also, as tested later, the presence of a diffusion contribution described by the Torrey's [27] or Vilfan and Zumer [28] theories would not improve the fits.

C. Analysis and discussion of the T_1 dispersion

The proton spin-lattice relaxation results were analyzed by means of a global nonlinear least-square minimization procedure in which Eqs. (1)–(4) were fitted simultaneously to all experimental T_1^{-1} data taking into account the expected relaxation mechanisms in each phase. In the isotropic phase, only the BPP contributions were assumed since collective movements are absent due to the uncorrelated molecular positions and orientations at long distance. In the mesophases, the additional contribution of layer undulations was included.

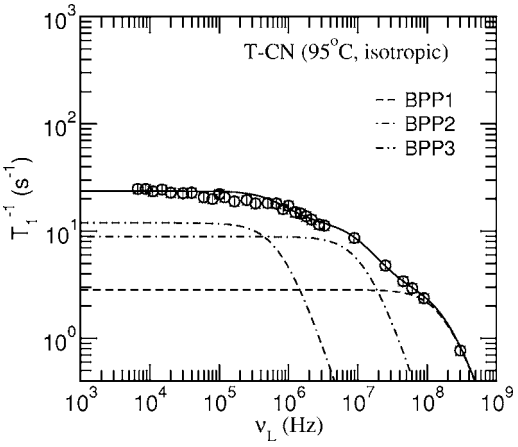

FIG. 8. Frequency dispersion of the proton spin-lattice relaxation rate T_1^{-1} in the isotropic phase (95 °C) of T-CN. The solid line is a fit of Eqs. (1)–(4), apart from the layer undulations contribution, to the experimental data. The three contributions of BPP-type are ascribed to local reorientations of the molecule, most probably of each dendrimer arm independently.

It turned out that the T-CN dispersions require at least three contributions of the BPP type to obtain a good fit of Eqs. (1)–(4) to the experimental data. The global fitted parameters are then: the three correlation times $\tau_{i,\infty}$, their activation energies W_i, and strengths of interaction A_{ROT1}, A_{ROT2}, A_{ROT3}, as well as A_{LU} and $\nu_{c\ \min}$, determining the contribution of layer undulations. The impact of $\nu_{c\ \max}$ on the LU dispersion curve is negligible in the kHz frequency range, its value was therefore fixed to 10^8 Hz. During the fitting procedure it was observed that the BPP1 contribution requires two different sets of $\tau_{1,\infty}$ and A_{ROT1} parameters, one for the results in the isotropic phase, another for the mesophase.

In Figs. 8–10 we present the T-CN experimental data and the dispersion curves resulting from the best global fit of Eqs. (1)–(4) at 95 °C, in the isotropic phase, at 70 °C, in the smectic-A phase, and at 43 °C, in the smectic-C phase. The

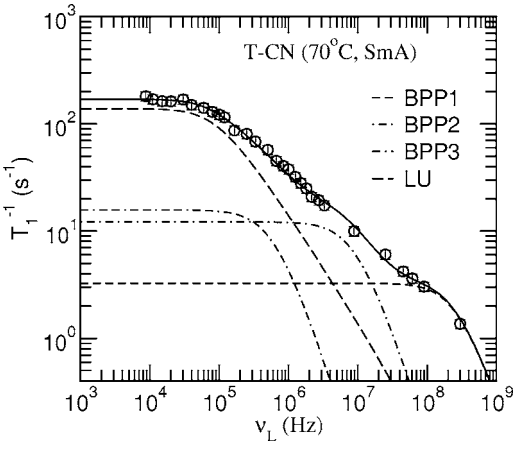

FIG. 9. Frequency dispersion of the proton spin-lattice relaxation rate T_1^{-1} in the smectic-A phase (70 °C) of T-CN. The solid line is a fit of Eqs. (1)–(4) to the experimental data. At frequencies below ~10 MHz a dispersion characteristic of layer undulations is well expressed.

fitted parameters are listed in Table II. We found that another set of parameters, obtained from the independent fits at each temperature separately, is quite compatible with the global fitted values within the accuracy of the fitting procedure.

An inspection of Figs. 8–10 shows that the experimental results are well explained by the proposed relaxation model. The three rotational modes, denoted as BPP1, BPP2, and BPP3, are associated with frequencies of the order of 10^9 Hz, 10^7 Hz to 10^8 Hz, and 10^6 Hz, corresponding to the correlation times given in Table II. Notably, the frequencies are above the frequency window investigated by dielectric measurements of Merkel *et al.* in a tetrapode with slightly larger molecular mass [9]. In the frequency range between 1 Hz and 10 MHz, dielectric spectroscopy detected the frequencies of the end-to-end reorientations of the whole tetrapode molecule, its precessional motion about the phase director, and rotation about the long molecular axis. Obviously, NMR covers the frequency range above the upper limit of dielectric spectroscopy. The rotational modes BPP1, BPP2, and BPP3 are, therefore, most probably associated with the dynamic processes of each dendrimer arm separately and independently of the other arms. Moreover, different values of $A_{\mathrm{ROT}i}$ indicate that different fractions of spins are relaxed by each of the modes, indirectly suggesting that, not only the dynamics of dendrimer arms but also individual motions of molecular groups, like siloxane, alkyl chain, or aromatic core, affect the relaxation of protons. This conjecture is supported by a rather weak temperature dependence of all three modes. Their fitted activation energies are $W_1 \sim 19$ kJ mol^{-1}, $W_2 \sim 13$ kJ mol^{-1}, and $W_3 \sim 12$ kJ mol^{-1}, probably too small to be associated with the motion of the entire tetrapode molecule. The small difference observed in the strength of the BPP1 relaxation mechanism (A_{ROT1}) between the isotropic and smectic phases may be caused by a more extended configuration of the dendrimer arm in the smectic-*A* and *C* phases. The values obtained for the correlation times τ_1 and τ_2 are within the range of values typically found for rotations/reorientations of low molecular mass liquid crystals [29]. In this way they corroborate the importance of monomeric units, i.e., of separate T-CN molecular entities, in the relaxation process. The rotation of the entire molecule around its long axis probably cannot be seen in the frequency window of our experiment, though its effect on the slowest of the BPP modes cannot be excluded.

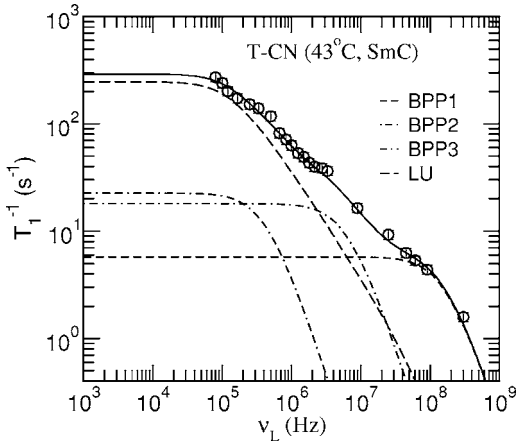

FIG. 10. Frequency dispersion of the proton spin-lattice relaxation rate T_1^{-1} in the smectic-*C* phase (43 °C) of T-CN. The solid line is a fit of Eqs. (1)–(4) to the experimental data.

The rotational modes determine the T-CN spin-lattice relaxation rate in the whole frequency range in the isotropic phase, and in the smectic phases above ~10 MHz. Below ~10 MHz, the T_1^{-1} dispersion in the smectic-*A* and *C* phases is clearly dominated by another relaxation mechanism, ascribed—in view of its specific frequency dependence $T_1^{-1} \propto \nu_L^{-1}$—to the undulations of smectic layers (LU). Notably, in the smectic-*A* phase a leveling-off of the LU dispersion occurs below ~100 kHz. The onset of the frequency independent plateau is well explained by the low frequency cut-off which limits the long wavelengths fluctuation modes. A similar cut-off could not be accessed in the smectic-*C* phase due to the experimental limiting conditions of the field-cycling spectrometer used in the present study. It should be mentioned that an attempt to describe the dispersion in the smectic phases by increasing the BPP3 contribution and diminishing the LU part failed completely. An exchange of the relative strengths of BPP3 and LU would make the global fit inconsistent and drastically reduce its quality.

A striking result of the present study is the well-expressed $T_1^{-1} \propto \nu_L^{-1}$ dispersion of layer undulations in the smectic phases. Such a behavior had been predicted years ago, but hardly observed in low molecular mass liquid crystals. It was reported to be observed only at frequencies below ~20 kHz, whereas at the intermediate frequencies, between 10 kHz and

TABLE II. Model fitting parameters obtained from the fits in the isotropic, smectic-*A*, and smectic-*C* phases of T-CN.

Phase (T)	I (95 °C)	I (90 °C)	SmA (70 °C)	SmA (60 °C)	SmC (43 °C)
$\tau_1 \times 10^{10}$ (s)	4.9	5.4	3.3	4.0	5.8
$\tau_2 \times 10^{9}$ (s)	7.2	7.7	9.9	11.4	14.7
$\tau_3 \times 10^{8}$ (s)	11.7	12.3	15.5	17.6	21.1
$A_{\mathrm{ROT1}} \times 10^{-9}$ (s^{-2})	1.2	1.2	2.0	2.0	2.0
$A_{\mathrm{ROT2}} \times 10^{-8}$ (s^{-2})	2.5	2.5	2.5	2.5	2.5
$A_{\mathrm{ROT3}} \times 10^{-7}$ (s^{-2})	2.0	2.0	2.0	2.0	2.0
$A_{\mathrm{LU}} \times 10^{-7}$ (s^{-2})	—	—	1.5	2.4	3.9
$\nu_{c\,\mathrm{min}} \times 10^{-4}$ (Hz)	—	—	6.7	6.9	7.1

10 MHz, the linear dispersion was lacking, being either too small or completely overlapped by the contribution of molecular translational self-diffusion [20–23]. In T-CN the translational diffusion of molecules is strongly hindered by the shape and size of the tetrapode and by the formation of dimers by dendrimer arms leaving thus the whole kHz frequency range open to the effect of layer undulations.

The fitted values of A_{LU} and $\nu_{c\ \mathrm{min}}$ in T-CN are larger than the ones reported for low molecular mass LCs. For example, A_{LU} in the smectic-*A* phase of T-CN is $\sim 2\times 10^7\ \mathrm{s}^{-2}$, whereas it is only $\sim 2\times 10^4\ \mathrm{s}^{-2}$ in a calamitic low molecular weight liquid crystal DB_8Cl [22]. Since both A_{LU} and $\nu_{c\ \mathrm{min}}$ are increasing with decreasing correlation lengths, parallel and perpendicular to the layers' normal, respectively, large values of A_{LU} and $\nu_{c\ \mathrm{min}}$ suggest considerably smaller correlation lengths if one assumes that the viscoelastic parameters in the mesogenic sublayers of T-CN are not drastically different from those found in low molecular mass LCs. Actually, the fitted value for A_{LU} allows one to obtain an estimate of the correlation length ξ, which measures the effective thickness of the coherently undulating smectic layers. The strength of the LU relaxation mechanism, A_{LU}, is given by the expression

$$\frac{9\gamma^4\hbar^2S^2k_BT}{64\pi K_1\xi}\frac{\overline{[3\cos^2(\alpha_{ij})-1]^2}}{r_{ij}^6},$$

where r_{ij} denotes the inter-proton distance of a spin pair ij, S is the orientational order parameter, and K_1 is the splay elastic constant of the mesogenic sublayer. Assuming typical values $r\sim 1.8$ Å, $S\sim 0.7$, and $K_1\sim 2\times 10^{-11}$ N, the estimated correlation length ξ is ~ 58 Å. This value is in excellent agreement with the layer thickness of T-CN, which is about 48 Å. It means that the sublayers of the mesogenic groups are undulating independently of each other, which may be expected in view of the micro-segregated structure of the T-CN smectic phases. Obviously, the siloxane moieties induce a mutual decoupling of the undulations performed by the sublayers of mesogenic groups. This conclusion is in agreement with earlier theoretical predictions that layer undulations represent a strong relaxation mechanism only when the interactions among neighboring layers can be neglected [24,30]. The above conclusion that the correlation length of undulations is of the order of layer thickness might seem contradictory to the high degree of smectic order as detected by x-ray diffraction (Sec. III A). However, the undulations detected by NMR are orientational fluctuations and occur presumably in the mesogenic sublayers which can be expected in view of the microsegregated structure of T-CN smectic phases. On the other hand, a high degree of smectic order detected by x-rays is static, positional order of molecules and refers to the whole smectic layers, composed of the siloxane moieties and mesogenic units. Therefore, the small correlation length of orientational fluctuations and, consequently, a decoupling of undulations between mesogenic sublayers is not incompatible with a high degree of positional smectic order, which extends over much larger distances.

IV. CONCLUSIONS

A new liquid crystalline organosiloxane tetrapode with cyano terminal polar groups, exhibiting smectic-*A* and smectic-*C* phases, was studied by x-ray diffraction, optical microscopy, and NMR proton spin-lattice relaxometry.

X-ray diffraction results show that a microsegregation of different molecular parts takes place in the smectic phases and that the arrangement is partially bilayered due to a certain degree of head-to-head association of dendrimer branches through their cyano end groups. The layer spacing is about ~ 48 Å at the SmA–SmC transition and increases with decreasing temperature in both phases indicating that the tilt angle in the smectic-*C* phase is relatively small. The fact that the second order x-ray diffraction line is clearly seen reflects a rather high degree of smectic positional order. The proposed packing model for T-CN is similar to that of low molecular mass organosiloxane liquid crystals. Obviously, the packing is governed by the micro-segregation effect characteristic of this kind of polyphilic molecules and, to a smaller extent, by the overall shape of the tetrapode.

Molecular dynamics in the isotropic and smectic phases of T-CN was investigated by measuring and analyzing the frequency dispersion of the proton spin-lattice relaxation rate T_1^{-1} at Larmor frequencies between 10 kHz and 300 MHz. In the isotropic phase, the relaxation is induced by at least three rotational modes associated with the independent motion of dendrimer arms. In the smectic-*A* and smectic-*C* phases, the dominating contribution of layer undulations with the typical frequency dependence $T_1^{-1}\propto\nu_L^{-1}$ is superimposed on the faster rotations of mesogenic units at frequencies below ~ 10 MHz. This result is particularly notable if compared to low molecular mass LCs where a frequency independent plateau, induced by molecular translational self-diffusion, is observed in the same frequency range. The reason for such behavior is two-fold. On one side, the intra- and inter-layer translational diffusion of T-CN molecules is strongly reduced due to the linking of mesogenic units to the central siloxane core and is therefore less important in the relaxation process. On the other side, the effectiveness of layer undulations in T-CN is larger than in ordinary smectic phases due to the mutual decoupling of mesogenic sublayers by the long flexible spacers and intermediate siloxane cores. Actually, a well-expressed T_1^{-1} contribution of layer undulations in thermotropic liquid crystals has been so far observed only in dendrimer systems.

ACKNOWLEDGMENTS

The authors acknowledge the financial support of the EU network on Super Molecular Liquid Crystal Dendrimers (RTN-LCDD)-HPRN-CT-2000-0001, and of the Portuguese-Slovenian bilateral project BI-PT-104-06-002. They thank Dr. G. Feio for the experimental help with the Bruker MSL spectrometer, Dr. D. Sousa and J. Cascais for the fast field-cycling NMR technical developments and support, and M. Cardoso for the help in the x-ray data analysis.

[1] G. R. Newkome, C. N. Moorefield, and F. Vögtle, *Dendrimers and Dendrons: Concepts, Syntheses, Applications* (Wiley-VCH, Weinheim, 2001).
[2] M. Ibn-Elhaj, A. Skoulios, D. Guillon, J. Newton, P. Hodge, and H. J. Coles, Liq. Cryst. **19**, 373 (1995); M. Ibn-Elhaj, A. Skoulios, D. Guillon, J. Newton, P. Hodge, and H. J. Coles, J. Phys. II **6**, 271 (1996).
[3] E. Corsellis, D. Guillon, P. Kloess, and H. Coles, Liq. Cryst. **23**, 235 (1997).
[4] T. Múrias, A. C. Ribeiro, D. Guillon, D. Shoosmith, and H. J. Coles, Liq. Cryst. **29**, 627 (2002).
[5] P. G. de Gennes and J. Prost, *The Physics of Liquid Crystals*, 2nd ed. (Oxford University Press, Oxford, 1993).
[6] V. Percec, W. D. Cho, and G. Ungar, J. Am. Chem. Soc. **119**, 1539 (2000).
[7] X. Zeng, G. Ungar, L. Yongsong, V. Percec, A. E. Dulcey, and J. K. Hobbs, Nature (London) **428**, 157 (2004).
[8] J.-M. Rueff, J. Barbera, B. Donnio, D. Guillon, M. Marcus, and J. L. Serrano, Macromolecules **36**, 8368 (2003).
[9] K. Merkel, A. Kocot, J. K. Vij, G. H. Mehl, and T. Meyer, Phys. Rev. E **73**, 051702 (2006).
[10] A. C. Ribeiro, P. J. Sebastião, and C. Cruz, Mol. Cryst. Liq. Cryst. Sci. Technol., Sect. A **363**, 291 (2001).
[11] D. M. Sousa, P. A. L. Fernandes, G. D. Marques, A. C. Ribeiro, and P. J. Sebastião, Solid State Nucl. Magn. Reson. **25**, 160 (2004); D. M. Sousa, G. D. Marques, P. J. Sebastião, and A. C. Ribeiro, Rev. Sci. Instrum. **74**, 4521 (2003).
[12] G. H. Mehl, A. J. Thornton, and J. W. Goodby, Mol. Cryst. Liq. Cryst. Sci. Technol., Sect. A **332**, 2965 (1999); S. Diez, D. Dunmur, M. R. De La Fuente, P. Karahaliou, G. Mehl, T. Meyer, M. A. Peréz Jubindo, and D. Photinos, Liq. Cryst. **30**, 1021 (2003); R. Elsäßer, G. H. Mehl, J. W. Goodby, and D. J. Photinos, Chem. Commun. (Cambridge) **10**, 851 (2000).
[13] C. B. McArdle, in *Side Chain Liquid Crystal Polymers* (Chapman and Hall, New York, 1989).
[14] D. Guillon and A. Skoulios, J. Phys. (France) **45**, 607 (1984).
[15] M. Ibn-Elhaj, H. J. Coles, D. Guillon, and A. Skoulios, J. Phys. II **3**, 1807 (1993).
[16] R. F. Boyer and R. L. Miller, Rubber Chem. Technol. **51**, 718 (1978).
[17] W. Woelfel, F. Noack, and M. Stohrer, Z. Naturforsch. A **30**, 437 (1975).
[18] R. Y. Dong, in *Nuclear Magnetic Resonance of Liquid Crystals*, 2nd ed. (Springer-Verlag, Berlin, 1997).
[19] R. Kimmich and E. Anoardo, Prog. Nucl. Magn. Reson. Spectrosc. **44**, 257 (2004).
[20] F. Noack, M. Notter, and W. Weiß, Liq. Cryst. **3**, 907 (1988); D. Pusiol and F. Noack, *ibid.* **5**, 377 (1989).
[21] P. J. Sebastião, A. C. Ribeiro, H. T. Nguyen, and F. Noack, Z. Naturforsch., A: Phys. Sci. **48**, 851 (1993); A. Ferraz, J. L. Figueirinhas, P. J. Sebastião, A. C. Ribeiro, H. T. Nguyen, and F. Noack, Liq. Cryst. **14**, 415 (1993); P. J. Sebastião, A. C. Ribeiro, H. T. Nguyen, and F. Noack, J. Phys. II **5**, 1707 (1995).
[22] A. Carvalho, P. J. Sebastião, A. C. Ribeiro, H. T. Nguyen, and M. Vilfan, J. Chem. Phys. **115**, 10484 (2001).
[23] E. Anoardo, F. Bonetto, and R. Kimmich, Phys. Rev. E **68**, 022701 (2003).
[24] B. Halle, Phys. Rev. E **50**, R2415 (1994).
[25] F. Bonetto, E. Anoardo, and R. Kimmich, J. Chem. Phys. **118**, 9037 (2003).
[26] R. Blinc, M. Luzar, M. Vilfan, and M. Burgar, J. Chem. Phys. **63**, 3445 (1975).
[27] H. C. Torrey, Phys. Rev. **92**, 962 (1953); F. Harmon and B. H. Muller, Phys. Rev. **182**, 400 (1969).
[28] M. Vilfan and S. Zumer, Phys. Rev. A **21**, 672 (1980).
[29] R. Y. Dong, Prog. Nucl. Magn. Reson. Spectrosc. **41**, 115 (2002).
[30] M. Vilfan, G. Althoff, I. Vilfan, and G. Kothe, Phys. Rev. E **64**, 022902 (2001).